Increasing and decreasing interregional brain coupling increases and decreases oscillatory activity in the human brain

Alejandra Sel[a,b,1], Lennart Verhagen[a,c], Katharina Angerer[a], Raluca David[a], Miriam C. Klein-Flügge[a], and Matthew F.S. Rushworth[a]

[a]Wellcome Centre for Integrative Neuroimaging, Department of Experimental Psychology, University of Oxford, Oxford OX1 3UD, United Kingdom; [b]Centre for Brain Science, Department of Psychology, University of Essex, Colchester CO4 3SQ, United Kingdom; and [c]Donders Institute for Brain, Cognition and Behaviour, Radboud University, 6525 HR Nijmegen, The Netherlands

Edited by Peter L. Strick, University of Pittsburgh, Pittsburgh, PA, and approved July 21, 2021 (received for review January 12, 2021)

The origins of oscillatory activity in the brain are currently debated, but common to many hypotheses is the notion that they reflect interactions between brain areas. Here, we examine this possibility by manipulating the strength of coupling between two human brain regions, ventral premotor cortex (PMv) and primary motor cortex (M1), and examine the impact on oscillatory activity in the motor system measurable in the electroencephalogram. We either increased or decreased the strength of coupling while holding the impact on each component area in the pathway constant. This was achieved by stimulating PMv and M1 with paired pulses of transcranial magnetic stimulation using two different patterns, only one of which increases the influence exerted by PMv over M1. While the stimulation protocols differed in their temporal patterning, they were comprised of identical numbers of pulses to M1 and PMv. We measured the impact on activity in alpha, beta, and theta bands during a motor task in which participants either made a preprepared action (Go) or withheld it (No-Go). Augmenting cortical connectivity between PMv and M1, by evoking synchronous pre- and postsynaptic activity in the PMv–M1 pathway, enhanced oscillatory beta and theta rhythms in Go and No-Go trials, respectively. Little change was observed in the alpha rhythm. By contrast, diminishing the influence of PMv over M1 decreased oscillatory beta and theta rhythms in Go and No-Go trials, respectively. This suggests that corticocortical communication frequencies in the PMv–M1 pathway can be manipulated following Hebbian spike-timing–dependent plasticity.

action control | transcranial magnetic stimulation | ventral premotor cortex | primary motor cortex | oscillations

The origins of oscillatory activity in the brain are currently an area of active debate, but common to many accounts is the idea that they partly reflect interaction or communication between brain areas (1, 2). Here, we directly test this possibility in the human brain by using manipulations that either increase or decrease the influence of one cortical area, the ventral premotor cortex (PMv), on another cortical area, the primary motor cortex (M1). Importantly we do this by carefully controlling for the impact on each component area when altering the strength of the pathway between them.

The PMv–M1 pathway is an ideal pathway in which to examine the effects of manipulating connection strength; it is well established that PMv exerts a powerful influence over M1 and that changes in connectivity are functionally relevant and correlated with motor control (3–9). Moreover, the pathway can be examined in humans; by stimulating PMv shortly (6 to 8 ms) before the stimulation of M1, it is possible to influence how activity in M1 evolves (8–12). Even though the impact of the first pulse in PMv is spatially circumscribed (13), it alters the activity in PMv neurons that project to M1 (3, 4, 6). When this is done repeatedly, the influence that PMv exerts over M1 is strengthened (7, 14, 15). Such a procedure is referred to as paired associative stimulation (PAS) or corticocortical PAS (ccPAS) when, as in this case, the two regions stimulated are areas of cortex. The evoked effects have been described as Hebbian in nature (16, 17, 18). If exactly the same amount of stimulation is applied to the same two areas but in the opposite temporal order, then the influence of PMv over M1 is, instead, diminished (14, 15). These effects have been established by examining changes in the coupling of blood oxygen level–dependent (BOLD) signals in PMv and M1 before and after ccPAS (15). From such experiments, it is clear that the increases and decreases in coupling that result from the two types of ccPAS are prominent between the stimulated areas themselves—PMv and M1—but they also extend to other motor association areas with which PMv and M1 are closely interconnected in the frontal and parietal cortex. The impact of ccPAS can also be visualized by measuring M1 excitability, which can be done by measuring motor-evoked potentials (MEPs) in hand muscles when single pulses of transcranial magnetic stimulation (TMS) are applied to M1 (14, 15). When this is done before and after ccPAS, M1 excitability increases in contexts, such as movement production, in which PMv normally exerts an excitatory influence over M1 (14, 15). Such effects are, however, context dependent, and in other settings in which PMv inhibits M1, it is this inhibitory action that is augmented by ccPAS (14).

CcPAS may, therefore, be an ideal tool for looking at the impact of manipulating coupling between two brain areas; if the

Significance

Oscillatory activity is prominent in the brain, and one hypothesis is that it is, in part, due to the nature of coupling or interaction patterns between brain areas. We tested this hypothesis by manipulating the strength of coupling between two brain regions (ventral premotor cortex, PMv, and motor cortex, M1) in two directions (increase or decrease) while carefully controlling for the impact each manipulation had on activity in each area. We looked at the PMv–M1 connection because it is the major cortical route by which prefrontal cortex might influence, inhibit, and curtail action-related activity in M1. Manipulating PMv–M1 coupling in accordance with Hebbian-like spike-timing–dependent plasticity resulted in changes in beta and theta frequencies linked to action control.

Author contributions: A.S. and M.F.S.R. designed research; A.S., K.A., and R.D. performed research; A.S., L.V., M.C.K.-F., and M.F.S.R. contributed new reagents/analytic tools; A.S., L.V., K.A., R.D., and M.C.K.-F. analyzed data; L.V., M.C.K.-F., and M.F.S.R. made comments on the paper; and A.S. and M.F.S.R. wrote the paper.

The authors declare no competing interest.

This article is a PNAS Direct Submission.

[1]To whom correspondence may be addressed. Email: alex.sel@essex.ac.uk.

This article contains supporting information online at https://www.pnas.org/lookup/suppl/doi:10.1073/pnas.2100652118/-/DCSupplemental.

Published September 10, 2021.

effects of two different ccPAS protocols are compared, then it should be possible to establish the effect of increasing or decreasing coupling between the two areas while holding constant the total amount of stimulation to each component area. We therefore examined the impact of either increasing or decreasing PMv–M1 coupling on electroencephalogram (EEG) oscillatory activity while human participants performed a simple Go/No-Go motor task in two blocks (referred to as Baseline and Expression blocks; Fig. 1). In participant group A, we applied 15 min of ccPAS over PMv followed by M1 (PMv–M1-ccPAS; each PMv pulse was followed by an M1 pulse at either 6- or 8-ms interpulse interval [IPI]). Before and after ccPAS, participants performed a Go/No-Go task in which participants responded to "Go" stimuli (blue square) and withheld responses to "No-Go" stimuli (red square). Furthermore, we investigated whether changes in oscillatory activity were dependent on ccPAS stimulation order by reversing the order of ccPAS stimulation (participant group B), that is, applying the first paired pulse over M1 and the second pulse over PMv (Fig. 1). Exactly the same number of pulses were applied to PMv and M1 in both participant groups A and B.

The use of a Go/No-Go task enabled us to look at a range of oscillatory effects in the EEG. Power increases in the beta range, called post-movement beta rebound, are related to activity in M1, and closely interconnected areas as movements are completed and should be observable on Go trials (19, 20). By contrast, activity in the theta range should be prominent on No-Go trials as in other situations that require the reorienting of behavior such as stopping an action from being made (21–25). Beta and theta band activity occurs in medial and lateral frontal and centroparietal areas that interact with PMv and adjacent inferior frontal cortex during action inhibition (10, 26–28). It is also possible to record activity in the alpha band in the EEG, although task-related modulations of alpha were less anticipated in a Go/No-Go task of this type. Given the difficulty of recording reliable gamma-band activity using EEG, we did not attempt to examine activity at this frequency.

Results

In experimental groups A (n = 16) and B (n = 17), we investigated, respectively, whether increasing or decreasing coupling across motor and motor association areas led to modulation of either fast (transient) or slow (sustained) EEG oscillatory dynamics associated with action control. We contrasted the effects of the two types of ccPAS, repeated paired stimulation of PMv followed by M1 (group A) or, vice versa, M1 followed by PMv (group B) on time-frequency oscillatory responses (computed as

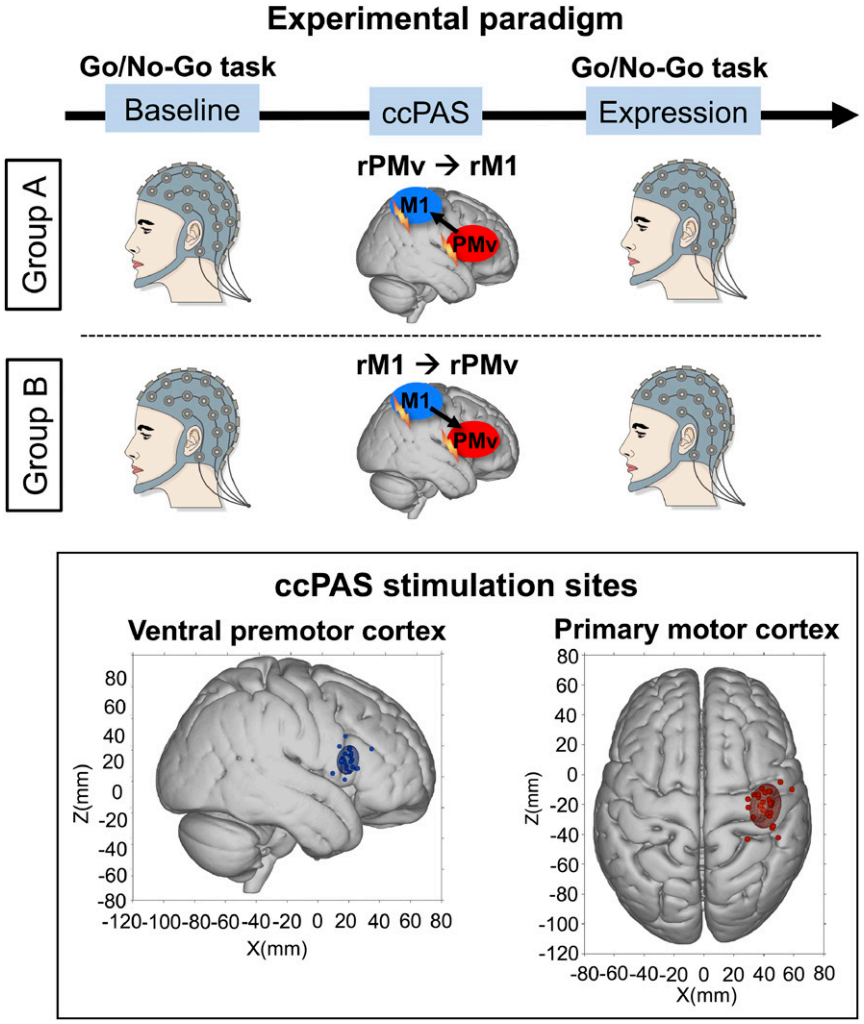

Fig. 1. Representation of the set up for groups A and B and individual subject scalp hotspot for rM1 and rPMv. (*Top*) Experimental design and setup for both experimental groups. The ccPAS period was preceded (Baseline) and followed (Expression) by Go/No-Go task blocks. EEG activity was recorded during the task blocks. (*Bottom*) Individual subject scalp hotspot (filled circles) and 95% group confidence ellipses for rM1 (red) and rPMv (blue) locations for the main and preliminary experiments in standardized MNI space.

Expression–Baseline block separately for Go and No-Go trials), recorded in a simple motor task.

Prior to starting the main experiment, in a preliminary investigation probing M1 excitability, we carried out two initial checks to ensure the effectiveness of the TMS protocol in the context of the current behavioral task (*SI Appendix*; Fig. S5*A*). First, we compared MEPs when we applied either single-pulse TMS (spTMS) over right M1 (16, 29) or paired-pulse TMS (ppTMS) over right PMv (conditioning pulse) followed by right M1 (8, 9, 14, 15). We recorded MEPs from the left first dorsal interosseus (FDI) muscle while participants performed Go trials in the Go/No-Go task. We demonstrated that PMv TMS did indeed alter the impact of M1 pulses on Go trials, confirming that the paired pulse procedure allowed us to probe the PMv–M1 pathway (*SI Appendix*; Fig. S5*B*). Second, we examined the impact of repeatedly inducing PMv activity either just before or just after inducing M1 activity during ccPAS. Again, we did this by measuring MEPs recorded in response to single pulses of M1 TMS on Go trials, but we did so before and after a 15-min period of ccPAS. Here, we demonstrated that we could manipulate the pathway's connectivity; the two ccPAS protocols used in groups A and B did indeed exert distinct effects on Go trials. While PMv–M1-ccPAS significantly enhanced the cortical excitability of M1 in Go trials, this M1 excitability remained the same after M1–PMv-ccPAS (*SI Appendix*; Fig. S5*C*).

Next, we examined the impact of the ccPAS in the EEG in groups A and B. We first compared the two groups of participants in the two groups before examining the changes occurring in each group in more detail. We focused on motor-relevant frequency bands theta, alpha, and beta (4 to 30 Hz) in frontocentral and centroparietal electrodes (*EEG Recording and Analysis*) known to reflect top-down control of motor processes likely to be relevant for performance of the Go/No-Go task (19–22, 30, 31). Because ccPAS can affect the motor system both ipsilaterally (14) and contralaterally (10), we examined a bilateral group of electrodes spanning both hemispheres.

We used cluster-based nonparametric permutation analysis procedures for identifying statistically significant clusters in the time, frequency, and spatial domain (*EEG Recording and Analysis*) (32–34). This revealed that ccPAS had a significant impact on motor-related beta and theta bands but little impact on the alpha band. Moreover, ccPAS effects significantly differed for Go and No-Go trials, and they diverged between the two participant groups (group A versus B—see *Materials and Methods* for a detailed explanation of analysis procedure). The significant effects of ccPAS were identified by the cluster-based permutation test as occurring in frequency bands typically regarded as being within the beta band range (19 to 24 Hz; Monte Carlo P value = 0.018) and within the theta band range (4 to 10 Hz; Monte Carlo P value = 0.008) between 0.15 and 1.2 s after the Go/No-Go stimulus onset.

Following these results, we contrasted the ccPAS effect, testing the difference across the two participant groups, for Go and No-Go trials separately, by subtracting EEG responses recorded at Baseline from Expression and contrasting this difference across groups (group A versus B) in the two types of trials. In the beta band, post hoc between-subject Student's t tests showed that the PMv–M1-ccPAS in group A led to an increase in beta synchronization only for Go trials (0.7 to 1.2 s after "Go" stimulus onset, consistent with the time of the post-movement beta rebound, PMBR) in the Expression versus the Baseline block. However, the opposite effects were found in Go trials when the ccPAS order was reversed in group B (Monte Carlo P value = 0.002, Fig. 2 *A*, *Left*). Note that, as we describe below, these differences could not be an indirect consequence of changes in reaction time because no changes in reaction time were apparent (*SI Appendix*, Table S2 and *Behavioral Results*). No significant differences in the beta band were observed for No-Go trials in the between-subject Student's t test analyses (Monte Carlo P value > 0.05) (Fig. 2 *A*, *Right*). In addition, we contrasted the ccPAS effects on beta activity recorded in the Baseline versus the Expression block for Go and No-Go trials separately for group A and B. The results of this within-subject Student's t test analysis revealed a late increase in beta synchronization after (versus before) PMv–M1-ccPAS for Go trials only (0.9 to 1.2 s after Go stimulus onset; Monte Carlo P value = 0.002, *SI Appendix*, Fig. S1, *Left*). By contrast, when the ccPAS order was reversed, changes in beta power were only observed in No-Go trials; beta responses first decreased before increasing in a later time window (0.3 to 1.1 s after No-Go stimulus onset; Monte Carlo P value = 0.0009, *SI Appendix*, Fig. S1, *Right*). No significant differences were seen in the beta band when comparing Baseline and Expression blocks for No-Go trials in group A, PMv–M1-ccPAS, nor for Go trials in group B, M1–PMv-ccPAS (Monte Carlo P value > 0.05). Furthermore, control analysis confirmed that the beta changes after the ccPAS manipulation in Go trials were not driven by group differences at baseline. Additional details of the results (mainly the data for each condition as opposed to the contrasts between conditions) and control analysis are shown in *SI Appendix*, Fig. S1 and *SI Appendix*.

The PMBR may reflect a short-lasting state of deactivation or "resetting" of premotor–motor networks after movement completion (35). The increased PMBR observed in Go trials during Expression may reflect an augmentation of active inhibition from PMv over M1 following strengthening of PMv's influence over M1 through ccPAS. The projections from PMv to M1 are excitatory, but many of these projections are onto inhibitory interneurons in M1 (36). Thus, PMv exerts both inhibitory and facilitatory influences over M1, and both of these influences can be augmented by PMv–M1-ccPAS (14). Moreover, the observation of the opposite effects on beta synchronization on Go trials, when reversing the order of the ccPAS stimulation in group B, are in line with previous evidence showing contrasting effects of reversed versus forward order ccPAS on M1 cortical excitability as well as on functional connectivity in motor networks (14, 15).

While the PMv–M1-ccPAS effects in the beta frequency occurred on Go trials, the theta effects occurred in No-Go trials in both groups. In No-Go trials, post hoc Student's t test analyses revealed that PMv-M1-ccPAS in group A led to a significant increase in theta power, whereas theta power decreased after reversed-order M1–PMv-ccPAS in group B (Monte Carlo P value = 0.002; 0.15 to 1.2 s after stimuli onset) (Fig. 3). In the same vein, the results of the post hoc within-subjects Student's t test analysis contrasting the ccPAS effects on theta activity between Baseline and Expression blocks revealed that the PMv-M1-ccPAS in group A led to a late increase of theta activation in No-Go trials (0.8 to 1.2 s after No-Go stimulus onset; Monte Carlo P value = 0.0009, *SI Appendix*, Fig. S2, *Top Right*), whereas the opposite effects in early theta activation were observed for No-Go trials after reversing ccPAS in group B (0.15 to 0.65 s after No-Go stimulus onset; Monte Carlo P value = 0.001, *SI Appendix*, Fig. S2, *Bottom Right*). Several findings have linked increased theta power in midfrontal regions to top-down executive control and action reprogramming during response conflict and motor inhibition, for example, after a No-Go command (21, 22). Notably, theta oscillatory changes increase with the level of response conflict, reflecting a larger top-down influence over motor circuits (31). It is clear that the inhibition of a specific action is associated with a series of interactions between medial frontal cortex areas such as the presupplementary motor area and PMv and possibly immediately adjacent tissue in the posterior inferior frontal cortex (10, 26, 27). Therefore, the increased theta power in No-Go trials after PMv–M1-ccPAS observed in experimental group A suggests augmentation of oscillatory activity associated with top-down motor control in response conflict, whereas the reversed-order M1–PMv-ccPAS suggests diminution of the same oscillatory activity in the same No-Go trials in experimental group B. No

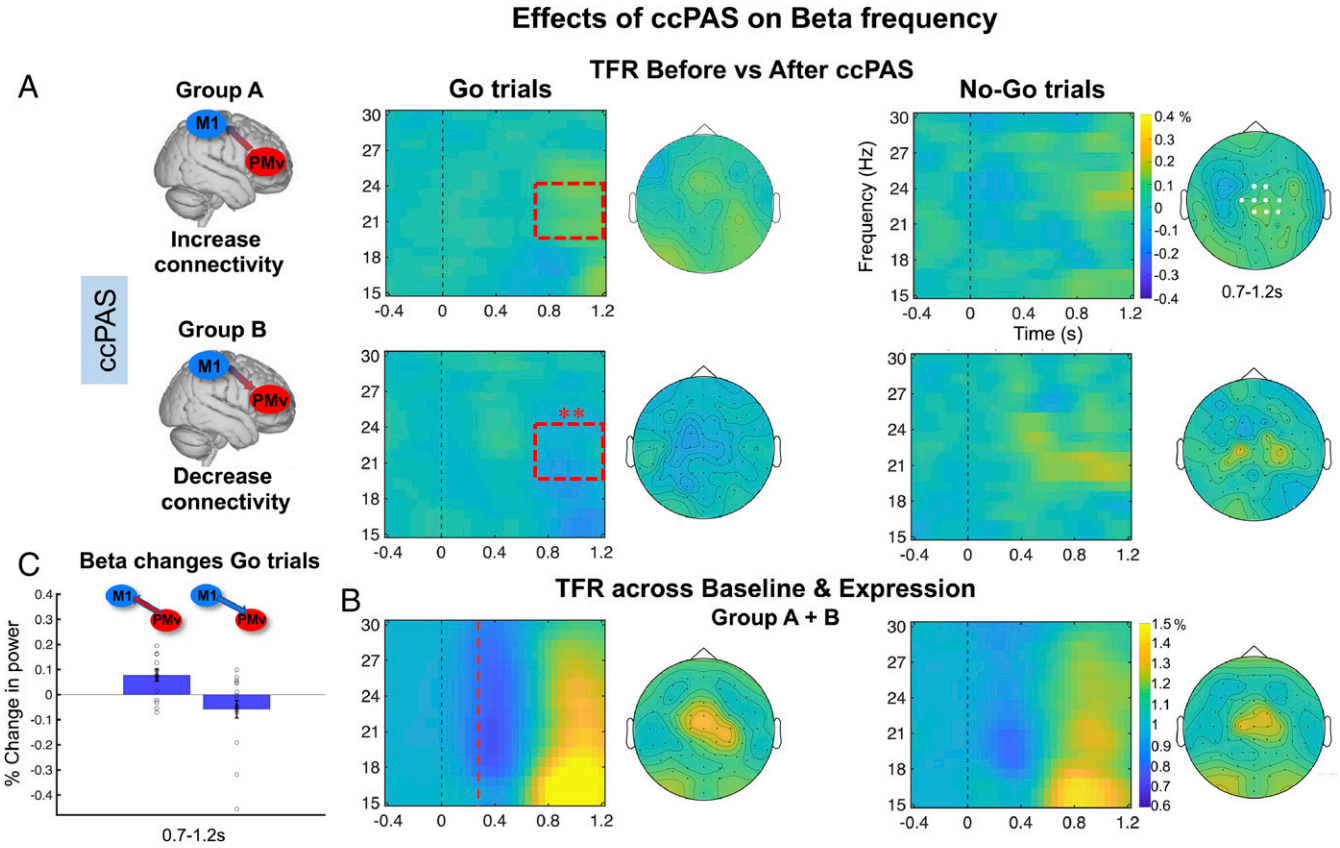

Fig. 2. EEG time-frequency responses in the beta band in frontocentral sites for Go and No-Go trials ($n = 33$). (*A* and *B*) EEG time-frequency responses (TFR) in the beta band (15 30 Hz) in frontocentral sites (C4, CZ, FC2, CP2, FCZ, C1, C2, FC4, CP4, and CPz; electrodes highlighted in white in *Top Right* topoplot) time locked to the onset of the Go/No-Go stimuli, computed as (*A*) the difference between Expression and Baseline blocks, (*B*) the mean of Baseline and Expression blocks collapsing across groups A + B. While *B* shows the PMBR effect was especially prominent in the Go trials, *A* illustrates how this changed as a function of the two types of ccPAS used in groups A and B. The dashed red square in *A* indicates the time window (0.7 to 1.2 s) in which significant modulation in beta responses after ccPAS were found. Dashed red line in *B* indicates the mean RT across Baseline and Expression for Go trials in both participant groups (mean = 352.36 s). (*C*) Mean beta frequency increase (PMv – M1 ccPAS) and decrease (M1 – PMv ccPAS) computed as the difference between Expression and Baseline in Go trials in the 0.7- to 1.2-s time window. Error bars represent SEM, single dots represent individual data points. In *A*, EEG TFR represent percentage change in power computed by subtracting the Baseline from the Expression block (0 = no percentage change). In *C*, EEG TFR represent relative percentage change in power with respect to the prestimulus interval (1 = no percentage change).

ccPAS effects on theta power were found in Go trials (Monte Carlo P value > 0.05) (Fig. 3). Moreover, control analysis confirmed that the theta changes after the ccPAS manipulation in No-Go trials were not driven by group differences at baseline. Further details of the results (mainly the data for each condition) and control analysis are shown in *SI Appendix*, Fig. S2 and *SI Appendix*.

We performed additional analyses to investigate the effects of ccPAS on nonstate-dependent oscillatory responses irrespective of motor state (i.e., collapsing across Go and No-Go trials). When contrasting the effects of PMv–M1-ccPAS in group A versus reversed M1–PMv-ccPAS in group B on cortical entrained motor activity (computed as the "Expression-minus-Baseline" difference), we found a lack of significant differences between the ccPAS manipulations (Monte Carlo P value > 0.05). This lack of difference between group A and B suggest that the direction of the stimulation, that is, PMv to M1 versus M1 to PMv, is ultimately driving the state-dependent effects observed in Go and No-Go trials. Furthermore, we investigated the absolute effect of PMv–M1- and reversed M1–PMv-ccPAS on activity recorded in Baseline versus Expression blocks. The analyses revealed that the ccPAS manipulation had a significant impact on motor-related theta, alpha, and beta (PMv–M1-ccPAS: 0.25 to 1.2 s after stimulus onset; 4 to 15 Hz; Monte Carlo P value = 0.004; M1–PMv-ccPAS: 0.25 to 1.1 s after stimulus onset; 9.9 to 14 Hz; Monte Carlo P value = 0.008; channels: C3, C4, CZ, FC1, FC2, CP1, CP2, FCZ, C1, C2, FC3, FC4, CP3, CP4, and CPZ). These results corroborate the absolute effect of the ccPAS manipulation on nonstate-dependent activations.

Oscillatory signals can reflect both transient, evoked activity and sustained, induced neural oscillations. Evoked responses are phase locked to external stimuli, whereas induced oscillations are not. PMv–M1-ccPAS manipulation led to long-latency oscillatory changes, whereas the reverse order led to frequency changes with an early onset. Thus, it is possible that these beta and theta modulations occurring after ccPAS reflect changes in either one or other neurophysiological mechanism or even a mixture of both mechanisms. In order to understand the nature of the ccPAS modulations, we carried out an analysis to identify any evoked oscillatory effects by computing the phase coherence across trials (i.e., intertrial linear coherence—ITLC) for each condition. First, we determined which parts of the Go/No-Go cue-related activity were evoked or sustained regardless of ccPAS. We observed phase coherence across all frequencies tested (4 to 30 Hz; Monte Carlo P value = 0.001) from 0.15 to 1.2 s after stimulus onset, but this was particularly obvious in the theta range during an early short-lived period around 0.3 s after stimulus presentation (*SI Appendix*, Fig. S3–yellow area in *Right*). In comparison to Go trials, No-Go trials were associated with stronger, transient, evoked activity in the theta band accompanied by milder sustained changes in alpha and beta activity (*SI Appendix*, Fig. S3—ITLC for all conditions

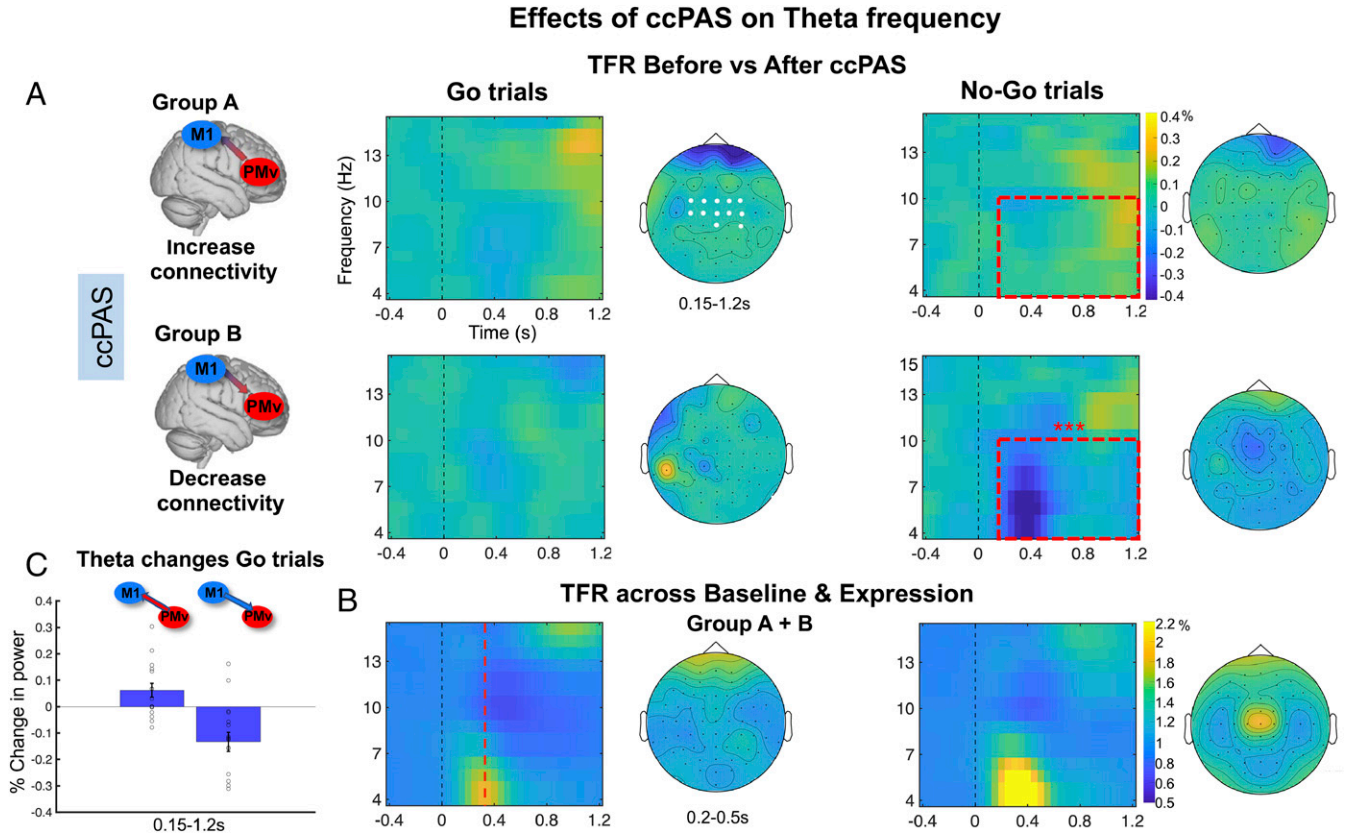

Fig. 3. EEG time-frequency responses in the theta band in frontocentral sites for Go and No-Go trials ($n = 33$). (*A* and *B*) EEG time-frequency responses in the theta band (4 to 15 Hz) in frontocentral sites (C3, C4, CZ, FC1, FC2, FCZ, C1, C2, FC3, FC4, CP4, and CPZ; electrodes highlighted in white in *Top Left* topoplot) time locked to the onset of the Go/No-Go stimuli, computed as (*A*) the difference between Expression and Baseline blocks, (*B*) the mean of Baseline and Expression blocks collapsing across groups A + B. While *B* shows the theta effect that was especially prominent in the No-Go trials, *A* illustrates how this changed as a function of the two types of ccPAS used in groups A and B. The dashed red square in *A* indicates the time window (0.15 to 1.2 s) in which a significant modulation in theta responses after ccPAS was found. The dashed red line in *B* indicates the mean RT across Baseline and Expression for Go trials in both participant groups (mean = 352.36 s). (*C*) Mean theta frequency increase (PMv – M1 ccPAS) and decrease (M1 – PMv ccPAS) computed as the difference between Expression and Baseline in No-Go trials in the 0.15- to 1.2-s time window. Error bars represent SEM, single dots represent individual data points. In *A*, EEG time-frequency responses represent percentage change in power computed by subtracting the Baseline from the Expression block (0 = no percentage change). In *C*, EEG time-frequency responses represent relative percentage change in power with respect to the prestimulus interval (1 = no percentage change).

tested). This analysis shows that some EEG changes are likely to be evoked responses that are phase locked to external stimuli even if later effects were likely to reflect induced oscillatory activity. We, therefore, next examined the impact of ccPAS to determine whether it affected only one type of activity or the other. We found that it modulated the amplitude of both early-evoked components as well as sustained changes of the theta oscillations in No-Go trials (Fig. 3 *A*, *Right*, dashed red line) and sustained changes in beta oscillations in Go trials (Fig. 2 *A*, *Left*, dashed red area). However, it did not modulate the phase consistency either in the theta or the beta band (*SI Appendix*, Fig. S3, comparable phase coherence between Baseline and Expression, before and after ccPAS, for Go/No-Go trials; Monte Carlo P value > 0.05). In summary, it is clear that the effects of ccPAS are not limited to an impact on evoked neural activity but include a clear effect on induced neural oscillations in both beta and theta bands. In the same vein, there were no significant differences in ccPAS effects on event-related potential (ERP) data between group A and B (*EEG Recording and Analysis* and *SI Appendix*, Fig. S4).

Discussion

The application of TMS pulses to PMv prior to TMS pulses to M1 evoke synchronous pre- and postsynaptic activity in the PMv-to-M1 pathway and alters the manner in which activity in M1 evolves (8–12, 37–39). Moreover, repeated paired stimulation of PMv followed by M1, PMv–M1-ccPAS leads to a subsequent state-dependent augmentation of PMv's influence over M1 expressed during action control (7, 14, 15). However, the same effects are not observed when M1 is stimulated prior to PMv in M1–PMv-ccPAS, and instead, such a protocol may even lead to a reduced influence of PMv over M1. These observations were replicated in the context of the current task (*SI Appendix*, Fig. S5). This means that ccPAS can be used to increase the interactions between two brain areas in order to examine the impact of connectivity change on oscillatory activity associated with the motor system. Importantly, the control ccPAS procedure, M1–PMv-ccPAS, comprises the same amount and intensity of both PMv and M1 stimulation as PMv–M1-ccPAS, and thus, it has the same impact on the component elements of the PMv–M1 circuit, but because of its different temporal patterning, it is associated with no augmentation of the influence of PMv over M1. This means that any change in oscillatory activity that is induced by PMv–M1-ccPAS that is not present with, or reversed with, M1–PMv-ccPAS cannot be attributed to the activation of either PMv or M1 but only to the manipulation of the connectivity between them.

Our results demonstrate that ccPAS delivered at rest leads to task-related changes in beta and theta oscillatory activity during action control. PMv–M1-ccPAS led to increased beta power in the PMBR in Go trials. Decreases and increases in beta frequency oscillations have, respectively, been linked to action initiation and cessation (40, 41), and the route between right PMv and adjacent inferior frontal cortex and M1 has been linked to both action initiation and inhibition (10, 11, 14, 26). In addition, PMv–M1-ccPAS led to increased theta power when there was greater demand for motor control in No-Go trials. While the changes occurred principally in the theta band, the fact that they occurred between 4 to 10 Hz meant that they extended into the low alpha band. Theta band activity occurs in medial and lateral frontal areas that interact with PMv and the adjacent inferior frontal cortex during action inhibition (10, 21, 22, 26, 27). These areas include the pre–supplementary motor area in the dorsal frontomedial cortex, PMv, the immediately adjacent cortex in the inferior frontal cortex, and M1 (10, 26, 27). It is increasingly clear that neurons concerned with the control of hand movements are present not just in PMv itself but in the inferior frontal cortex anterior to PMv (42) and that PMv receives a strong monosynaptic projection from many parts of prefrontal cortex including inferior frontal regions (43, 44).

By contrast, the opposite beta and theta patterns were seen after reversed-order M1–PMv stimulation in group B. The reversed-order M1–PMv stimulation protocol is unlikely to lead to simultaneous pre- and postsynaptic activity in the PMv–M1 pathway; as a result, connectivity in the pathway should either remain constant or, more likely, decrease (14, 15). More generally, according to the principles of Hebbian-like spike timing–dependent plasticity (16), the firing of presynaptic cells before postsynaptic cells leads to long-term potentiation, whereas the firing of postsynaptic activity before presynaptic activity usually induces long-term depression. In tandem, results from group A and B demonstrate that it is possible to entrain the cortical oscillatory dynamics of action control by repeated stimulation of a directed projection in a specific motor circuit. They also suggest that transmission of causal influences between PMv and M1 is linked to state-dependent channels of communication tuned to specific frequencies, specifically, the beta rhythm for action initiation and cessation on Go trials and the theta rhythm for action inhibition on No-Go trials. Different cortical rhythms in the beta and theta range are associated with distinct functional roles in motor control and inhibition (23, 25).

PMv–M1-ccPAS selectively modulated induced beta oscillatory activity at the time of movement completion (there was no evidence for stimulus-locked evoked beta responses). This suggests that PMv exerts an influence over M1 that is associated with resonant activity in the beta range (19, 20). In contrast, reversed-order M1–PMv-ccPAS led to moderate PMBR reductions. Although there are strong projections from PMv to M1, projections from M1 to PMv also exist (43). The moderate decrease of PMBR after M1–PMv-ccPAS may, therefore, reflect not just a reduction in influence exerted by PMv over M1 but a change in the projections in the opposite direction. Interestingly, the beta band effects of ccPAS were most apparent at the time of increased synchronization when movements were completed rather than at the time of desynchronization when movements were being initiated. Similar to neurons in M1, neurons in PMv also project directly to the spinal cord (45). Therefore, the increased synchronization at the time of movement completion may reflect not only plasticity changes in the motor cortex but also changes on the descending projections to the spinal cord. Future studies should investigate the potential premotor origin of these PMBR after the ccPAS manipulation. In addition to induced neural oscillations in the beta range, it is possible that ccPAS also affects short-lasting beta-burst activity only visible on single trials during movement initiation (46). Further research in the future might investigate the effects of ccPAS on the trial-to-trial dynamics of action control.

Theta band power increases have been suggested as spectral fingerprints of top-down executive control (21–25, 30, 31, 47). Here, we observed increased theta oscillations in No-Go trials after PMv–M1-ccPAS, suggesting greater top-down motor control during response conflict as a result of entrainment of PMv–M1 connections. Opposite effects on theta oscillations are observed after reversed-order M1–PMv-ccPAS, suggesting decreased executive control over motor output. Notably, while the ccPAS may cause some changes in early-evoked and later-induced theta activity (Fig. 3), these modulations cannot be explained by changes in phase-locked responses (*SI Appendix*, Fig. S3) or in ERP components (*SI Appendix*, Fig. S4). Instead, the ccPAS appears to affect the amplitude of oscillatory activity linked to response inhibition. The results are also consistent with previous investigations emphasizing theta oscillatory activity in integrative mechanisms and as mediators of information transfer between prefrontal and motor areas in decision-making and action control (23–25).

Given the clear influence of ccPAS on beta and theta oscillations during action performance and inhibition, changes in task performance might, therefore, also have been expected. Changes in task performance after ccPAS have been reported in both the visual and motor system (7, 48). Despite conducting a number of analyses (*Behavioral Analysis*), we were unable to find robust evidence for such changes in the current study (*SI Appendix*, *Behavioral Results*). The task was chosen for its simplicity, and it is possible that ccPAS-induced changes in performance might only have been seen in more demanding tasks as has been previously reported (7). Another possibility is that the effects of the ccPAS manipulation on behavior might not be most apparent immediately after the stimulation. Further future studies should investigate the possibility of longer-term influence of ccPAS on either speed or accuracy rates. As it stands, however, the oscillatory changes induced by ccPAS in the current setting can be interpreted as a direct result of the ccPAS rather than a secondary consequence of ccPAS-induced changes in task performance. The current findings complement previous evidence of oscillatory changes at rest after ccPAS (49) and of selective enhancement of functional specific pathways outside the PMv–M1 network (50)

It is notable that the ccPAS procedure induced a suite of changes that were apparent at several different points in time after Go and No-Go cues. The modulatory effect of ccPAS on a beta oscillatory activity and theta oscillatory were apparent 700 and 150 ms after Go and No-Go stimuli, respectively, approximately during the same period when beta and theta oscillations appeared most robustly in the baseline state in our study (Figs. 2 and 3). The ccPAS also produced changes in MEPs following application of spTMS to M1 125 ms after Go cues (*SI Appendix*, Fig. S5*C*). The 125-ms time point was examined because it is close to times at which PMv has been shown to influence M1 in previous studies (10, 11, 37), but it is possible that additional effects might have been observed had we tested other time points after the Go cue.

In summary, corticocortical communication frequencies in the human PMv–M1 pathway can be manipulated, leading to state-dependent changes during action control. The frequency-specific patterns of oscillatory activity change found after different types of ccPAS on Go versus No-Go trials reflects spectral fingerprints of augmentation versus reduction of top-down PMv influence over M1. The patterns are consistent with Hebbian-like (16) spike timing–dependent long-term potentiation and depression and with hierarchical models of action control in which top-down motor control occurs in tandem with oscillations with specific resonant properties in the beta and theta frequency ranges (23, 25).

Materials and Methods

Participants. A total of 36 healthy, right-handed adults participated across the two experimental groups. Three participants were excluded due to excessive noise in the EEG signal, resulting in 33 participants—16 in group A (23.75 ± 4.59; 10; 0.81 ± 0.17) and 17 in group B (22.64 ± 2.31; 5; 0.93 ± 0.13)

(where numbers correspond to mean age ± SD; number of female participants, handiness mean ± SD; as measured by the Edinburgh handedness inventory, adapted from ref. 51). All participants had no personal or familial history of neurological or psychiatric disease, were right handed (except for one participant—handiness score 0.045), were screened for adverse reactions to TMS and risk factors by means of a safety questionnaire, and received monetary compensation for their participation. Participants underwent high-resolution, T1-weighted structural MRI scans. Sample sizes were determined based on previous studies that have used the same ccPAS protocol to measure the influence of PMv over M1 cortical excitability (14, 15) and studies that have used the Go/No-Go paradigm to investigate oscillatory responses during action control in humans. All participants gave written informed consent, and all the experimental procedures were approved by the Medical Science Interdivisional Research Ethics Committee (Oxford, No. R29477/RE004).

Experimental Design. Both experimental groups started with a Baseline block, followed by a ccPAS period, and an Expression block (Fig. 1). During Baseline and Expression blocks, participants performed a visual Go/No-Go task. Trials started with the presentation of either a blue (Go trials—70% of trials) or a red (No-Go trials) square (1.8 × 1.8 cm) displayed for 500 ms. These were followed by a yellow fixation cross (1.3 × 1.3 cm) presented centrally on the screen for a time interval between 2 and 3 s. There was a total of 304 trials per block (equal number of trials in the Baseline and the Expression blocks) with a short break halfway through the block. Blocks always started with four consecutive Go trials. Participants were instructed to press a button with their left index finger as soon as the blue square was presented and to withhold the response when the red square appeared on the screen. Reaction times and accuracy were recorded. During the task, participants were seated at ∼50 cm from the screen in a sound and electrically shielded booth.

In the two experimental groups, the ccPAS period that intervened between Baseline and Expression blocks consisted of 15 min of ccPAS over PMv and M1 applied at 0.1 Hz (90 total stimulus pairings) with an IPI of either 6 or 8 ms. Both resting-state and task-state interactions between M1 and PMv, and adjacent areas, emerge at 6- to 8-ms intervals (8, 9, 14, 15). Precise interpulse timing is critical if both PMv and M1 pulses are to produce coincident influences on corticospinal activity. Therefore, we employed an IPI of 8 ms when testing half of the participants in group A and in group B and an IPI of 6 ms in the other half of participants in each group. The impact of this difference in the experimental manipulation was tested by a repeated-measures ANOVA with within-subject factors block (Baseline, Expression) and trial type (Go, No-Go), between-subject factor ccPAS order (PMv–M1-ccPAS, M1–PMv-ccPAS), and the IPI (8 ms, 6 ms) as a covariate. No effects of the 6-ms IPI versus 8-ms IPI was seen even when the analysis focused on the time window and frequency bands in which the key effects of ccPAS on neural oscillations had been found (Monte Carlo P values > 0.05). Because these analyses found no effect of the 2-ms difference, we do not consider this difference in IPI further. In the experimental group A, the pulse applied to PMv always preceded the pulse over M1, while the opposite was true in experimental group B, which served as an active control.

Corticocortical-Paired Associative Stimulation. ccPAS was applied using two Magstim 200 stimulators, each connected to 50-mm figure eight–shaped coils. The M1 "scalp hotspot" was the scalp location where the TMS stimulation evoked the largest left FDI MEP amplitude. This scalp location was projected onto high-resolution, T1-weighted MRIs of each volunteer's brain using frameless stereotactic neuronavigation (Brainsight; Rogue Research). In contrast to the scalp hotspot, the right M1 "cortical hotspot" was the mean location in the cortex where the stimulation reached the brain for all participants in Montreal Neurological Institute (MNI) coordinates (X = 41.03 ± 6.59, Y = −16.74 ± 9.35, Z = 63.69 ± 8.20; Fig. 1—cortical coordinates computed using Brainsight stereotactic neuronavigation for each participant; mean cortical coordinates computed by averaging all individual's cortical coordinates). These coordinates were similar to that reported previously (9, 11, 14, 15). The PMv coil location was determined anatomically as follows. A marker was placed on each individual's MRI and adjusted with respect to individual sulcal landmarks to a location immediately anterior to the inferior precentral sulcus. The mean MNI cerebral location of the PMv stimulation was at X = 59.66 ± 3.41, Y = 17.07 ± 6.28, Z = 14.85 ± 8.50 (Fig. 1) and lies within the region defined previously as human PMv (rostral part) and the adjacent inferior frontal gyrus (posterior/mid part) (52), more precisely over areas 44d and 44v of the pars opercularis within the inferior frontal gyrus (53), which resembles parts of macaque PMv in cytoarchitecture and connections (54, 55).

Resting motor threshold (RMT) of the right M1 (mean ± SD, 43.13 ± 7.22% stimulator output) was determined as described previously (56). As in previous ccPAS studies (14, 15), PMv TMS was proportional to RMT—110% (47.76 ± 7.35). M1 stimulation intensity during the experiment was set to elicit single-pulse MEPs of ±1 mV (47.23 ± 7.58% stimulator output). TMS coils were positioned tangential to the skull, with the M1 coil angled at ∼45° (handle pointing posteriorly) and the PMv coil at ∼0° relative to the midline (handle pointing anteriorly). The PMv coil was fixed in place with an adjustable metal arm and monitored throughout the experiment. The M1 coil was held by the experimenter. Left FDI electromyography activity was recorded with bipolar surface Ag-AgCl electrode montages. Responses were band-pass filtered between 10 and 1.000 Hz, with additional hardwired 50-Hz notch filtering (CED Humbug), sampled at 5,000 Hz, and recorded using a CED D440-4 amplifier, a CED micro1401 Mk.II A/D converter, and PC running Spike2 (Cambridge Electronic Design). All trials with muscle preactivation between Go/No-Go onset and TMS pulse were offline discarded.

EEG Recording and Analysis. EEG was recorded with sintered Ag/AgCl electrodes from 64 scalp electrodes mounted equidistantly on an elastic electrode cap (64Ch-Standard-BrainCap for TMS with Multitrodes; EasyCap). All electrodes were referenced to the right mastoid and re-referenced to the average reference offline. Continuous EEG was recorded using NuAmps digital amplifiers (Neuroscan, 1000-Hz sampling rate).

Offline EEG analysis was performed using FieldTrip (33). The data were down sampled to 500 Hz and digitally band-pass filtered between 1 to 40 Hz. Bad/missing channels were restored using a FieldTrip-based spline interpolation. Next, the data were segmented into 3.5-s intervals starting from 1.4 s before stimulus onset. This was done for Go and No-Go trials separately, and incorrect trials and trials in which reaction times (RTs) were too slow or too fast (± 2SD) were excluded from the analysis. Automatic artifact rejection was performed excluding trials and channels whose variance (z-scores) across the experimental session exceeded a threshold of 10. This was combined with visual inspection for all participants eliminating large technical and movement-related artifacts. Physiological artifacts such as eye blinks and saccades were corrected by means of independent component analysis (RUNICA, logistic Infomax algorithm) as implemented in the FieldTrip toolbox. Those independent components (7.22 on average across participants; 4.8 SD) whose timing and topography resembled the characteristics of the physiological artifacts were removed. For the ERP analysis, the signal was re-referenced to the arithmetic average of all electrodes, and segments were baseline corrected using an interval from 500 to 100 ms before the stimulus onset.

For the time-frequency analysis, single-subject activations for each block (Baseline, Expression) and trial type (Go, No-Go) were averaged and submitted to a complex multitaper time-frequency transformation from 4 to 30 Hz in steps of 1 Hz, with a fixed Hanning window of 0.75 s. A relative Baseline normalization was performed using a time window from −1.1 to 0 s in respect to stimulus onset. To estimate the effects of the ccPAS protocol on neural responses of action control in the Go/No-Go task, time-frequency activations time locked to stimulus onset were computed at the group level using a nonparametric randomization test controlling for multiple comparisons (32). Investigations of the neural dynamics of cognitive and motor control processes highlight the functional significance of both low- and high-frequency oscillations in action performance and inhibition. Theta (4 to 8 Hz), alpha (9 to 12 Hz), and beta (13 to 30 Hz) spectrums have all been linked to aspects of action control. Therefore, in the statistical analyses, no frequency bands were selected a priori. Instead, the statistical analyses were performed on all motor-relevant frequency bands (4 to 30 Hz) and across the entire time window in which oscillatory changes associated with motor control have been observed—0.2 to 1.2 s after stimulus onset. Statistical analyses were restricted to 15 electrodes distributed over frontocentral and centroparietal areas, that is, FC3, FC1, FCZ, FC2, FC4, C3, C1, CZ, C2, C4, CP3, CP1, CPZ, CP2, and CP4, where the neural phenomena linked to motor control are typically distributed (57–59).

To test if the ccPAS protocol influenced cortical correlates of action control and if this influence happened in a state-dependent manner (Go versus No Go), we used a cluster-based permutation approach as implemented in FieldTrip (see below). Since this method allows the comparison of only two conditions, we first computed the "cortical entrained effect" (calculated by the subtraction of each frequency at each time point of activity recorded in Baseline from the Expression block) for Go and No-Go trials separately. We then calculated the difference of the cortical entrained effect between No-Go trials versus Go trials. Thereafter, we contrasted the "No-Go-minus-Go cortical entrained effect" recorded from the participants that received PMv–M1-ccPAS (group A; n = 16) versus the participants that received reverse-order M1–PMv-ccPAS (group B; n = 17) by means of between-subject nonparametric cluster-based permutation analysis. A nonparametric cluster-based permutation approach is an efficient way of dealing with the multiple comparison problem that prevents biases in preselecting time windows or frequency bands avoiding inflation of type I error rate (32, 60). Time-frequency responses in all

conditions are represented in *SI Appendix*, Fig. S1 (beta band) and *SI Appendix*, Fig. S2 (theta band). In addition, we used the same cluster-based permutation approach to investigate the effect of ccPAS on all trial types, irrespectively of the motor state (i.e., across Go and No-Go trials), by contrasting activity recorded in the Baseline and Expression period for experimental group A and B.

Subject-wise time-frequency courses were extracted at the selected electrodes and were passed to the statistical analysis procedure in FieldTrip, the details of which are described by Maris and Oostenveld (32). Subject-wise time-frequency courses were compared to identify statistically significant clusters in the time, frequency, and spatial domain using a FieldTrip-based analysis across all time points and frequency bands focusing on frontocentral and centroparietal sites described above (33). FieldTrip uses a nonparametric method (34) to address the multiple comparison problem. T-values of adjacent temporal and frequency points whose *P* values were less than 0.05 were clustered by adding their t-values, and this cumulative statistic is used for inferential statistics at the cluster level. This procedure, that is, the calculation of t-values at each temporal point followed by clustering of adjacent t-values, was repeated 5,000 times, with randomized swapping and resampling of the subject-wise time-frequency activity before each repetition. This Monte Carlo method results in a nonparametric estimate of the *P* value representing the statistical significance of the identified cluster.

In addition, to rule out the possibility that changes in oscillatory activity after ccPAS were linked to phase-locked responses to stimulus presentation, we computed the phase coherence across trials (ITLC) for each condition (*SI Appendix*, Fig. S3). We tested the effects of ccPAS on ITLC, mimicking the cluster-based permutation analysis performed on time-frequency oscillatory responses across all time points and frequency bands focusing on the 15 electrodes distributed over frontocentral and centroparietal areas, that is, FC3, FC1, FCZ, FC2, FC4, C3, C1, CZ, C2, C4, CP3, CP1, CPZ, CP2, and CP4.

For the ERP analysis, single-subject ERPs for each block (Baseline, Expression) and trial type (Go, No-Go) were calculated and used to compute ERP grand averages across subjects (*SI Appendix*, Fig. S4). The analysis on the ERP data mimicked the time-frequency analysis. In brief, ERP activations time locked to stimulus onset were computed at the group level using a nonparametric randomization test controlling for multiple comparisons (32). To test the effects of ccPAS on ERPs related to action control, we first computed the ccPAS effect on ERPs (by the subtraction of each time point of the trials in the Baseline block from the Expression block) for Go and No-Go trials. We then computed the difference of the ccPAS effect between No-Go and Go trials. Finally, we contrasted the "No-Go-minus-Go ccPAS effect" between the two participant groups (PMv–M1-ccPAS group versus reversed-order PMv–M1-ccPAS group) by means of between-subject nonparametric cluster-based permutation analysis. Statistical analyses were done across the entire time window in which the N2-P3 component typically takes place, this is, 0.2 to 0.6 s (28), and it was restricted to 15 electrodes distributed over frontocentral and centroparietal areas (see above). Subject-wise activation time courses were extracted at the selected electrodes and were passed to the analysis procedure of FieldTrip (32). The cluster-based permutation analysis on the ERP data did not find any significant differences in the cortical entrained effect between the participant groups A and B at any electrode cluster when contrasting either Go or No-Go trials (Monte Carlo *P* values > 0.05). These results demonstrated that 1) the effects of ccPAS on the PMv–M1 circuit are frequency specific and only affect particular oscillatory bands linked to action control, that is, beta and theta bands, and 2) the changes observed in the slow-frequency band theta cannot be explained by changes in the ERP components. There was, however, a significant difference between Go versus No-Go trials across both groups, confirming that the action control manipulation was effective (Monte Carlo *P* value = 0.001; electrode sites—C4, C3, CZ, FC1, FC2, CP1, CP2, FCZ, C1, C2, FC3, CP3, CP4, and CPZ; between 0.20 and 0.50 s after stimulus onset; *SI Appendix*, Fig. S4).

Behavioral Analysis. Behavioral performance measures comprised median RTs (excluding trials with RT ± 2SD from the mean, 3.9%) and accuracy (excluding omission errors in Go trials, 5%, and commission errors to No-Go trials, 12%). We tested the effect of the ccPAS protocol on RTs and accuracy measures. A repeated-measures ANOVA using the within-subject factors of block (Baseline, Expression) and trial type (Go, No-Go) and the between-subject factor of ccPAS order (PMv–M1-ccPAS, M1–PMv-ccPAS) was used to analyze the behavioral data of groups A and B. No main effects or interactions in accuracy or reaction time were found (all *P*s > 0.05). We also examined if the difference in IPI (6 ms IPI versus 8 ms) influenced RTs and accuracy measures. We used the same ANOVA with the same variables and added the IPI (6 ms IPI versus 8 ms) as a covariate. We did not find an influence of IPI difference on RTs or accuracy (all *P*s > 0.05). Moreover, we tested the effects of ccPAS on overall accuracy across all Go and No-Go trials in two Student's *t* tests (Baseline versus Expression) separately for group A and B. Again, no effects of ccPAS on overall accuracy was found (all *P*s > 0.05)

In addition, we explored the possibility that EEG modulations (computed as the difference between Baseline and Expression blocks for Go and No-Go trials separately) could be linked to participants' performances (median RT in Go trials and accuracy rates in Go and No-Go trials) at Baseline. No relationship was found between participants' median RT/accuracy and EEG changes between the Baseline versus Expression blocks neither in group A nor group B (Monte Carlo *P* value > 0.05). We also tested if undergoing ccPAS influenced the aftereffects of No-Go trials on subsequent Go trials. We found that there were aftereffects of No-Go trials on subsequent Go trials represented by slower median RTs in the Expression versus Baseline period for both experimental groups A and B ($F(1,31) = 7.746$, $P = 0.009$, $\eta p^2 = 0.2$), possibly due to fatigue.

Data Availability. Anonymized human brain, physiological, and behavioral data have been deposited in Open Science Framework (DOI: 10.17605/OSF.IO/6VTFB) (61).

ACKNOWLEDGMENTS. This study was funded by the Bial Foundation to A.S. (Grant 44/16), John Templeton Foundation Prime Award (15464/ Subaward Ref. SC14), and Wellcome Trust: WT100973AIA to M.F.S.R. We would like to thank Nadescha Trudel for her help in data collection.

1. P. Fries, Rhythms for cognition: Communication through coherence. *Neuron* **88**, 220–235 (2015).
2. F. van Ede, A. J. Quinn, M. W. Woolrich, A. C. Nobre, Neural oscillations: Sustained rhythms or transient burst-events? *Trends Neurosci.* **41**, 415–417 (2018).
3. H. Shimazu, M. A. Maier, G. Cerri, P. A. Kirkwood, R. N. Lemon, Macaque ventral premotor cortex exerts powerful facilitation of motor cortex outputs to upper limb motoneurons. *J. Neurosci.* **24**, 1200–1211 (2004).
4. G. Cerri, H. Shimazu, M. A. Maier, R. N. Lemon, Facilitation from ventral premotor cortex of primary motor cortex outputs to macaque hand muscles. *J. Neurophysiol.* **90**, 832–842 (2003).
5. A. Kraskov, G. Prabhu, M. M. Quallo, R. N. Lemon, T. Brochier, Ventral premotor-motor cortex interactions in the macaque monkey during grasp: Response of single neurons to intracortical microstimulation. *J. Neurosci.* **31**, 8812–8821 (2011).
6. G. Prabhu *et al*., Modulation of primary motor cortex outputs from ventral premotor cortex during visually guided grasp in the macaque monkey. *J. Physiol.* **587**, 1057–1069 (2009).
7. F. Fiori, E. Chiappini, A. Avenanti, Enhanced action performance following TMS manipulation of associative plasticity in ventral premotor-motor pathway. *Neuroimage* **183**, 847–858 (2018).
8. M. Davare, R. Lemon, E. Olivier, Selective modulation of interactions between ventral premotor cortex and primary motor cortex during precision grasping in humans. *J. Physiol.* **586**, 2735–2742 (2008).
9. M. Davare, K. Montague, E. Olivier, J. C. Rothwell, R. N. Lemon, Ventral premotor to primary motor cortical interactions during object-driven grasp in humans. *Cortex* **45**, 1050–1057 (2009).
10. F. X. Neubert, R. B. Mars, E. R. Buch, E. Olivier, M. F. Rushworth, Cortical and subcortical interactions during action reprogramming and their related white matter pathways. *Proc. Natl. Acad. Sci. U.S.A.* **107**, 13240–13245 (2010).
11. E. R. Buch, R. B. Mars, E. D. Boorman, M. F. Rushworth, A network centered on ventral premotor cortex exerts both facilitatory and inhibitory control over primary motor cortex during action reprogramming. *J. Neurosci.* **30**, 1395–1401 (2010).
12. M. Davare, A. Kraskov, J. C. Rothwell, R. N. Lemon, Interactions between areas of the cortical grasping network. *Curr. Opin. Neurobiol.* **21**, 565–570 (2011).
13. M. C. Romero, M. Davare, M. Armendariz, P. Janssen, Neural effects of transcranial magnetic stimulation at the single-cell level. *Nat. Commun.* **10**, 2642 (2019).
14. E. R. Buch, V. M. Johnen, N. Nelissen, J. O'Shea, M. F. Rushworth, Noninvasive associative plasticity induction in a corticocortical pathway of the human brain. *J. Neurosci.* **31**, 17669–17679 (2011).
15. V. M. Johnen *et al*., Causal manipulation of functional connectivity in a specific neural pathway during behaviour and at rest. *eLife* **4**, e04585 (2015).
16. G. Koch, V. Ponzo, F. Di Lorenzo, C. Caltagirone, D. Veniero, Hebbian and anti-Hebbian spike-timing-dependent plasticity of human cortico-cortical connections. *J. Neurosci.* **33**, 9725–9733 (2013).
17. Y. Z. Huang *et al*., Plasticity induced by non-invasive transcranial brain stimulation: A position paper. *Clin. Neurophysiol.* **128**, 2318–2329 (2017).
18. A. Suppa *et al*., The associative brain at work: Evidence from paired associative stimulation studies in humans. *Clin. Neurophysiol.* **128**, 2140–2164 (2017).
19. M. T. Jurkiewicz, W. C. Gaetz, A. C. Bostan, D. Cheyne, Post-movement beta rebound is generated in motor cortex: Evidence from neuromagnetic recordings. *Neuroimage* **32**, 1281–1289 (2006).

20. L. M. Parkes, M. C. Bastiaansen, D. G. Norris, Combining EEG and fMRI to investigate the post-movement beta rebound. *Neuroimage* **29**, 685–696 (2006).
21. T. Tsujimoto, H. Shimazu, Y. Isomura, K. Sasaki, Theta oscillations in primate prefrontal and anterior cingulate cortices in forewarned reaction time tasks. *J. Neurophysiol.* **103**, 827–843 (2010).
22. T. Tsujimoto, H. Shimazu, Y. Isomura, Direct recording of theta oscillations in primate prefrontal and anterior cingulate cortices. *J. Neurophysiol.* **95**, 2987–3000 (2006).
23. R. F. Helfrich, A. Breska, R. T. Knight, Neural entrainment and network resonance in support of top-down guided attention. *Curr. Opin. Psychol.* **29**, 82–89 (2019).
24. R. F. Helfrich, R. T. Knight, Cognitive neurophysiology of the prefrontal cortex. *Handb. Clin. Neurol.* **163**, 35–59 (2019).
25. R. F. Helfrich *et al*., Neural mechanisms of sustained attention are rhythmic. *Neuron* **99**, 854–865.e5 (2018).
26. A. R. Aron, T. W. Robbins, R. A. Poldrack, Inhibition and the right inferior frontal cortex: One decade on. *Trends Cogn. Sci.* **18**, 177–185 (2014).
27. A. R. Aron, T. E. Behrens, S. Smith, M. J. Frank, R. A. Poldrack, Triangulating a cognitive control network using diffusion-weighted magnetic resonance imaging (MRI) and functional MRI. *J. Neurosci.* **27**, 3743–3752 (2007).
28. R. J. Huster, S. Enriquez-Geppert, C. F. Lavallee, M. Falkenstein, C. S. Herrmann,Electroencephalography of response inhibition tasks: Functional networks and cognitive contributions. *Int. J. Psychophysiol.* **87**, 217–233 (2013).
29. F.-X. Neubert, R. B. Mars, E. Olivier, M. F. Rushworth, Modulation of short intracortical inhibition during action reprogramming. *Exp. Brain Res.* **211**, 265–276 (2011).
30. J. Harper, S. M. Malone, E. M. Bernat, Theta and delta band activity explain N2 and P3 ERP component activity in a go/no-go task. *Clin. Neurophysiol.* **125**, 124–132 (2014).
31. K. Yamanaka, Y. Yamamoto, Single-trial EEG power and phase dynamics associated with voluntary response inhibition. *J. Cogn. Neurosci.* **22**, 714–727 (2010).
32. E. Maris, R. Oostenveld, Nonparametric statistical testing of EEG- and MEG-data. *J. Neurosci. Methods* **164**, 177–190 (2007).
33. R. Oostenveld, P. Fries, E. Maris, J.-M. Schoffelen, FieldTrip: Open source software for advanced analysis of MEG, EEG, and invasive electrophysiological data. *Comput. Intell. Neurosci.* **2011**, 156869 (2011).
34. E. T. Bullmore *et al*., Global, voxel, and cluster tests, by theory and permutation, for a difference between two groups of structural MR images of the brain. *IEEE Trans. Med. Imaging* **18**, 32–42 (1999).
35. G. Pfurtscheller, A. Stancák Jr, C. Neuper, Post-movement beta synchronization. A correlate of an idling motor area? *Electroencephalogr. Clin. Neurophysiol.* **98**, 281–293 (1996).
36. H. Tokuno, A. Nambu, Organization of nonprimary motor cortical inputs on pyramidal and nonpyramidal tract neurons of primary motor cortex: An electrophysiological study in the macaque monkey. *Cereb. Cortex* **10**, 58–68 (2000).
37. C. Catmur, R. B. Mars, M. F. Rushworth, C. Heyes, Making mirrors: Premotor cortex stimulation enhances mirror and counter-mirror motor facilitation. *J. Cogn. Neurosci.* **23**, 2352–2362 (2011).
38. F. Fiori *et al*., Long-latency interhemispheric interactions between motor-related areas and the primary motor cortex: A dual site TMS study. *Sci. Rep.* **7**, 1–10 (2017).
39. F. Fiori *et al*., Long-latency modulation of motor cortex excitability by ipsilateral posterior inferior frontal gyrus and pre-supplementary motor area. *Sci. Rep.* **6**, 1–11 (2016).
40. Y. Zhang, Y. Chen, S. L. Bressler, M. Ding, Response preparation and inhibition: The role of the cortical sensorimotor beta rhythm. *Neuroscience* **156**, 238–246 (2008).
41. S. Picazio *et al*., Prefrontal control over motor cortex cycles at beta frequency during movement inhibition. *Curr. Biol.* **24**, 2940–2945 (2014).
42. I. Caprara, E. Premereur, M. C. Romero, P. Faria, P. Janssen, Shape responses in a macaque frontal area connected to posterior parietal cortex. *Neuroimage* **179**, 298–312 (2018).
43. R. P. Dum, P. L. Strick, Frontal lobe inputs to the digit representations of the motor areas on the lateral surface of the hemisphere. *J. Neurosci.* **25**, 1375–1386 (2005).
44. E. Borra, M. Gerbella, S. Rozzi, G. Luppino, Anatomical evidence for the involvement of the macaque ventrolateral prefrontal area 12r in controlling goal-directed actions. *J. Neurosci.* **31**, 12351–12363 (2011).
45. R. P. Dum, P. L. Strick, Motor areas in the frontal lobe of the primate. *Physiol. Behav.* **77**, 677–682 (2002).
46. J. R. Wessel, β-Bursts reveal the trial-to-trial dynamics of movement initiation and cancellation. *J. Neurosci.* **40**, 411–423 (2020).
47. A. N. Landau, P. Fries, Attention samples stimuli rhythmically. *Curr. Biol.* **22**, 1000–1004 (2012).
48. V. Romei, E. Chiappini, P. B. Hibbard, A. Avenanti, Empowering reentrant projections from V5 to V1 boosts sensitivity to motion. *Curr. Biol.* **26**, 2155–2160 (2016).
49. D. Veniero, V. Ponzo, G. Koch, Paired associative stimulation enforces the communication between interconnected areas. *J. Neurosci.* **33**, 13773–13783 (2013).
50. E. Chiappini, J. Silvanto, P. B. Hibbard, A. Avenanti, V. Romei, Strengthening functionally specific neural pathways with transcranial brain stimulation. *Curr. Biol.* **28**, R735–R736 (2018).
51. R. C. Oldfield, The assessment and analysis of handedness: The Edinburgh inventory. *Neuropsychologia* **9**, 97–113 (1971).
52. M. A. Mayka, D. M. Corcos, S. E. Leurgans, D. E. Vaillancourt, Three-dimensional locations and boundaries of motor and premotor cortices as defined by functional brain imaging: A meta-analysis. *Neuroimage* **31**, 1453–1474 (2006).
53. F.-X. Neubert, R. B. Mars, A. G. Thomas, J. Sallet, M. F. Rushworth, Comparison of human ventral frontal cortex areas for cognitive control and language with areas in monkey frontal cortex. *Neuron* **81**, 700–713 (2014).
54. P. L. Croxson *et al*., Quantitative investigation of connections of the prefrontal cortex in the human and macaque using probabilistic diffusion tractography. *J. Neurosci.* **25**, 8854–8866 (2005).
55. M. Petrides, G. Cadoret, S. Mackey, Orofacial somatomotor responses in the macaque monkey homologue of Broca's area. *Nature* **435**, 1235–1238 (2005).
56. P. M. Rossini *et al*., Non-invasive electrical and magnetic stimulation of the brain, spinal cord and roots: Basic principles and procedures for routine clinical application. Report of an IFCN committee. *Electroencephalogr. Clin. Neurophysiol.* **91**, 79–92 (1994).
57. R. J. Huster, S. Enriquez-Geppert, C. F. Lavallee, M. Falkenstein, C. S. Herrmann, Electroencephalography of response inhibition tasks: Functional networks and cognitive contributions. *Int. J. Psychophysiol.* **87**, 217–233 (2013).
58. S. Enriquez-Geppert, C. Konrad, C. Pantev, R. J. Huster, Conflict and inhibition differentially affect the N200/P300 complex in a combined go/nogo and stop-signal task. *Neuroimage* **51**, 877–887 (2010).
59. P. D. Gajewski, M. Falkenstein, Effects of task complexity on ERP components in Go/Nogo tasks. *Int. J. Psychophysiol.* **87**, 273–278 (2013).
60. A. Keil *et al*., Committee report: Publication guidelines and recommendations for studies using electroencephalography and magnetoencephalography. *Psychophysiology* **51**, 1–21 (2014).
61. A. Sel, Increasing and decreasing inter-regional brain coupling increases and decreases oscillatory activity in the human brain. Open Science Framework. 10.17605/OSF.IO/6VTFB. Deposited 26 August 2021.